HHS Public Access

Author manuscript

Clin Cancer Res. Author manuscript; available in PMC 2024 February 01.

Published in final edited form as:

Clin Cancer Res. 2023 February 01; 29(3): 548–559. doi:10.1158/1078-0432.CCR-22-2566.

A Phase II Window of Opportunity Study of Neoadjuvant PD-L1 versus PD-L1 plus CTLA-4 Blockade for Patients with Malignant Pleural Mesothelioma

Hyun-Sung Lee[1], **Hee-Jin Jang**[1], **Maheshwari Ramineni**[2], **Daniel Y. Wang**[3], **Daniela Ramos**[1], **Jong Min Choi**[1], **Taylor Splawn**[1], **Monica Espinoza**[1], **Michelle Almarez**[1], **Leandria Hosey**[1], **Eunji Jo**[4], **Susan Hilsenbeck**[4], **Christopher I. Amos**[5], **R. Taylor Ripley**[6], **Bryan M. Burt**[1,*]

[1.]Systems Onco-Immunology Laboratory, David J. Sugarbaker Division of Thoracic Surgery, Michael E. DeBakey Department of Surgery, Baylor College of Medicine, Houston, TX 77030, USA.

[2.]Department of Pathology and Immunology, Baylor College of Medicine, Houston, TX 77030.

[3.]Section of Hematology and Oncology, Department of Medicine, Baylor College of Medicine, Houston, TX 77030, USA.

[4.]Advanced Technology Cores, Dan L. Duncan Comprehensive Cancer Center, Baylor College of Medicine, Houston, Texas, USA.

[5.]Institute for Clinical and Translational Research, Baylor College of Medicine, Houston, TX

[6.]David J. Sugarbaker Division of Thoracic Surgery, Michael E. DeBakey Department of Surgery, Baylor College of Medicine, Houston, TX 77030, USA.

Abstract

Purpose: We report the results of a phase 2, randomized, window-of-opportunity trial of neoadjuvant durvalumab versus durvalumab plus tremelimumab followed by surgery in patients with resectable malignant pleural mesothelioma (MPM)(NCT02592551).

[*]**Corresponding author:** Bryan M. Burt, M.D., Systems Onco-Immunology Laboratory, David J. Sugarbaker Division of Thoracic Surgery, Michael E. DeBakey Department of Surgery, Baylor College of Medicine, One Baylor Plaza, Houston, TX 77030, USA. Tel: 713-798-8266. bryan.burt@bcm.edu.

AUTHOR CONTRIBUTIONS

H.S.L., H.J.J., and B.M.B. conceived the study and contributed to the study design, data analysis, interpretation, and writing. M.R., D.Y.W., E.J., and S.H. contributed to the study design and data analysis. D.R., J.M.C., T.S., M.E., L.H., and M.A. contributed to data collection. C.I.A. and R.T.R. contributed to data interpretation and manuscript editing. H.S.L. and B.M.B contributed to funding acquisition.

All other authors declare no potential conflicts of interest.

DECLARATION OF INTERESTS

• HSL reports research funding from the Cancer Prevention Research Institute of Texas and clinical research funding from Samyang Biopharm.

• DYW reports clinical trial funding from Tessa Therapeutics and is a consultant for Regeneron and Sanofi Genzyme.

• RTR reports research support from the National Institutes of Health and the American Association for Thoracic Surgery, and is a non-remunerated director on the board of the Mesothelioma Applied Research Foundation.

• BMB reports research funding from the National Institute of Health, Cancer Prevention Research Institute of Texas; clinical trial funding from AstraZeneca, Novartis, and Momotaro-Gene; and has been a speaker for AstraZeneca (molecular targeted therapy for lung cancer).

Patients and Methods: The primary objective was alteration of the intratumoral CD8/Treg ratio after combination immune checkpoint blockade (ICB) therapy. Secondary and exploratory objectives included other changes in the tumor microenvironment, survival, safety, tumor pathologic response (PR), and systemic immune responses.

Results: Nine patients received monotherapy and 11 received combination therapy. Seventeen of the 20 patients (85%) receiving ICB underwent planned thoracotomy. Both ICB regimens induced CD8 T cell infiltration into MPM tumors but did not alter CD8/Treg ratios. At 34.1 months follow-up, patients receiving combination ICB had longer median overall survival (not reached) compared to those receiving monotherapy (14.0 months). Grade ≥3 immunotoxicity occurred in 8% of patients in the monotherapy group and 27% of patients in the combination group. Tumor PR occurred in 6 of 17 patients receiving ICB and thoracotomy (35.3%), among which major PR (>90% tumor regression) occurred in 2 (11.8%). Single-cell profiling of tumor, blood, and bone marrow revealed that combination ICB remodeled the immune contexture of MPM tumors; mobilized $CD57^+$ effector memory T cells from the bone marrow to the circulation; and increased the formation of tertiary lymphoid structures in MPM tumors that were rich in $CD57^+$ T cells.

Conclusions: These data indicate that neoadjuvant durvalumab plus tremelimumab orchestrates *de novo* systemic immune responses that extend to the tumor microenvironment and correlate with favorable clinical outcomes.

Keywords

malignant pleural mesothelioma; neoadjuvant immunotherapy; immune checkpoint blockade; tertiary lymphoid structures; systems onco-immunology

INTRODUCTION

Malignant pleural mesothelioma (MPM) is an aggressive malignancy of the pleura that invades the heart, lungs, and abdominal viscera, and is fatal in most cases. Less than ten percent of individuals diagnosed with MPM are alive 5 years later and median survival without therapy is 7 months.[1–4] Combination pemetrexed and cisplatin is first-line chemotherapy for MPM and increases median survival from 9.3 to 12.1 months compared with cisplatin alone.[5] The anti-angiogenic agent bevacizumab was reported to increase survival by 2 months when added to pemetrexed/cisplatin,[6] however it has not been approved by the United States Food and Drug Administration (FDA). Radiation is limited by the large field size that is required to treat MPM tumors, but is used in multimodal settings.[7, 8] Whereas surgery alone does not meaningfully improve survival, multimodal approaches incorporating surgery in select patients result in median survival of 14–19 months.[1, 9, 10]

Early phase trials of immune checkpoint blockade (ICB) against programmed cell death-1 (PD-1)/programmed cell death-ligand 1 (PD-L1) alone or in combination against cytotoxic T-lymphocyte–associated antigen-4 (CTLA-4) have been promising in the salvage setting for patients with unresectable MPM.[11–17] Recently, the phase III CheckMate 743 trial demonstrated that combination ICB with nivolumab plus ipilimumab improved overall survival (OS) for patients with untreated, unresectable MPM compared with platinum/

pemetrexed chemotherapy,[18,19] and this front-line regimen was approved by the FDA for unresectable MPM. We designed a prospective, randomized trial with window-of-opportunity design to compare the impact of neoadjuvant durvalumab (anti-PD-L1) with durvalumab plus tremelimumab (anti-CTLA-4) on the tumor immune contexture of patients with resectable MPM.

MATERIALS and METHODS

Trial Oversight.

The protocol and all modifications were approved by the Institutional Review Board at Baylor College of Medicine (H-36952) and were conducted in accordance with the Declaration of Helsinki and International Conference on Harmonization Good Clinical Practice guidelines. All patients provided written informed consent before enrollment. Durvalumab and tremelimumab were provided by the sponsor, AstraZeneca/MedImmune, which played no other role in the study or report.

Study Design

This was a phase II, prospective, randomized window-of-opportunity trial completed at Baylor College of Medicine that enrolled patients with surgically resectable MPM (NCT02592551). Eligible patients underwent a staging procedure that included cervical mediastinoscopy with mediastinal lymph node biopsies and diagnostic laparoscopy with peritoneal lavage and peritoneal biopsies. Thoracoscopy with tumor biopsies was performed for the purpose of this trial. Patients without pathologic nodal or peritoneal disease were randomly assigned in a 2:2:1 ratio to receive one dose of durvalumab (10mg/kg i.v.), 2) one dose of durvalumab (1500 mg) plus one dose of tremelimumab (75 mg i.v.), or 3) no ICB. The no ICB group was included as a reference for survival metrics, only. Randomization strata included histology (epithelioid *vs.* non-epithelioid [sarcomatoid or biphasic]) and receipt of prior chemotherapy (yes *vs.* no). ICB was administered 3 days to 3 weeks following the staging procedure and surgical resection was performed 3 to 6 weeks after ICB by extended pleurectomy/decortication (P/D) or extrapleural pneumonectomy (EPP) (Figure 1A). Macroscopic complete resection (MCR) is considered the objective of resectional surgery for MPM and is most commonly defined as removal of all grossly visible and palpable tumor.[20] Heated intraoperative chemotherapy (HIOC) was permitted immediately after tumor resection as a 1-hour lavage of cisplatin (175–225 mg/m^2) at 42°C per our standard protocol.[21] Tumor and blood were obtained before and after ICB (at thoracoscopy and resection, respectively) and the 6th rib was obtained to analyze bone marrow responses to ICB when it was removed to facilitate surgical exposure.

The primary objective of the study was change in the ratio of intratumoral cytotoxic T cells to regulatory T cells (CD8/Treg) in the combination ICB group, which was hypothesized to increase in response to effective ICB either through expansion of intratumoral cytotoxic T cells and/or contraction of regulatory T cells. Secondary objectives included alteration of tumor PD-L1 expression and ICOS$^+$ CD4 T cells after ICB, and comparisons of OS and disease-free survival (DFS) between groups. Exploratory objectives included determination of adverse events (AEs), rates of tumor pathologic responses, alteration of intratumoral

and circulating immune cell populations following ICB, and comparisons of post-ICB bone marrow cell populations between monotherapy and combination therapy groups. OS was defined as time to death following enrollment. DFS was defined as time to recurrence in patients undergoing MCR, or time to progression in patients who were not able to undergo surgery or those that underwent less than MCR. Progression was evaluated every 3 months by CT and supported by PET-CT and/or biopsy as clinically indicated.

To investigate intratumoral responses to ICB, tumor tissues were obtained from the lateral pleura both before and after ICB. At the time of thoracoscopy, a small incision was made on the lateral aspect of the thorax at a site in line with the future thoracotomy, and thoracoscopic biopsies were performed from the lateral pleura. At thoracotomy, tumor tissue was obtained from a similar, albeit previously unmanipulated region of the lateral pleura (Figure 1B), and the thoracoscopy site was excised. To investigate pathologic response, tumor tissue was also obtained from this lateral pleural region, and additionally from one to two other regions (apical and/or basilar), depending on the presence of macroscopically visible tumor in these regions.

Participants

Eligible patients were 18 years of age or older and had epithelioid or non-epithelioid (biphasic or sarcomatoid) MPM that was considered to be surgically resectable. Resectability was determined by thoracic surgeons and defined as MPM confined to the ipsilateral hemithorax and physiologic capacity to tolerate resection. Key inclusion required Eastern Cooperative Oncology Group performance status of 0 or 1 and adequate organ and bone marrow function. Patients receiving prior chemotherapy to downstage radiographic N2 disease were eligible. Key exclusion criteria were pathologic nodal metastases or peritoneal extension of disease, immunodeficiency, and ongoing systemic immunosuppressive therapy. Target enrollment was 8 patients in the monotherapy group and 8 patients in the combination therapy group who had tumor tissue and blood collected before and after ICB, and 4 patients in the no ICB group.

Determination of sample size.

The primary outcome in this study is a change in the ratio of CD8/Treg before and after treatment with combination durvalumab plus tremelimumab within subjects. There are no data available to estimate a change in the ratio of CD8/Treg before and after the treatment, but in our pilot data from twelve subjects with MPM, the log-transformed ratio of CD8/Treg was approximately normally distributed with a mean of 6.96 and standard deviation of 2.24. Assuming that repeat values are moderately correlated (γ=0.5), the difference between before and after the combination treatment will also have a standard deviation of 2.24. We estimated that we would have 80% power (alpha=5%, a paired t-test) to detect an increased log-ratio CD8/Treg of 17.71 after the combination treatment with 8 subjects.

Statistical Analysis.

Student’s t-tests or Mann-Whitney U tests compared continuous variables, and χ^2 or Fisher’s exact tests compared categorical variables. Survival curves were generated by the Kaplan-Meier method, and intergroup comparisons were performed by log-rank test.

Univariable Cox regression was used to determine associations with OS or DFS. Z values of protein markers were calculated by subtracting average protein expression from raw data for each protein and dividing by its standard deviation. Mean metal intensities (MMI) of proteins were compared with t-tests. IMC and CyTOF data were analyzed with FlowJo® V10.7.2 (FlowJo, OR). Statistical analyses were performed with Prism® 8.0 (GraphPad Software, CA) or SPSS 28.0 (SPSS, IL), all tests were two-tailed, and significance was considered as $P<0.05$.

Data Availability

The data supporting the findings of the present study are available within the paper and its supplementary information files. All requests for raw and analyzed data and materials are promptly reviewed by the Clinical Trial Support Unit at the Dan L Duncan Comprehensive Cancer Center's Biomedical Informatics Group at Baylor College of Medicine to verify if the request is subject to any intellectual property or confidentiality obligations. Source data for the TCGA tumor samples were retrieved from The Cancer Genome Atlas (TCGA) portal (https://portal.gdc.cancer.gov/). mRNA sequencing data of the 211 samples in Brigham and Women's Hospital was extracted from the European Genome-phenome Archive under accession code EGAS00001001563. Original mRNA expression data deposited in the National Center for Biotechnology Information's Gene Expression Omnibus (GEO) database (GSE29211) were also used. Patient-related data not included in the paper were generated as part of clinical trials and may be subject to patient confidentiality. All other relevant de-identified data related to the present study are available from the corresponding author (B.B.) upon reasonable academic request and will require the researcher to sign a data access agreement with Baylor College of Medicine after approval.

RESULTS

Patients

From May 2016 through September 2019, 44 patients consented to the trial and screened for eligibility. Twenty patients were deemed screen failures and 24 patients were enrolled. Nine patients were randomized to monotherapy with durvalumab, 11 to combination therapy with durvalumab and tremelimumab, and 4 to no ICB. A CONSORT diagram of enrollment is shown in Supplementary Figure 1 and characteristics of randomized patients are shown in Table 1 and Supplementary Table 1. Among the 24 eligible patients, 16 (66.7%) had epithelioid tumor histology and 8 (33.3%) had non-epithelial tumor histology. Among the 8 patients with non-epithelial histology 4 (50%) had biphasic tumor histology, and 4 (50%) had sarcomatoid tumor histology. Seventy-five percent of patients were male, 100% had clinical stage I-II MPM, 12.5% had prior chemotherapy, and 21% had tumor PD-L1 expression >50%.

Operative Course

Among the 20 patients that received ICB, 17 underwent thoracotomy for curative-intent surgery. In these patients, the median interval between ICB and thoracotomy was 22 days (range, 14–61 days) and surgery was not delayed in any case. Three patients that received ICB did not have thoracotomy, owing to declining performance status (n=1), occurrence of

non-ST elevation myocardial infarction (n=1), or tumor progression (n=1). Each of these patients was enrolled with clinical stage I disease, and none were thought to have adverse events to ICB.

Of the 8 patients that received monotherapy and thoracotomy, 6 patients had MCR (4 by P/D and 2 by EPP), 1 had a partial P/D for intraoperative findings of mediastinal invasion, and 1 had exploratory thoracotomy (ET) without tumor resection for intraoperative findings of diffuse chest wall invasion. Of the 9 patients that received combination therapy and thoracotomy, 6 patients had MCR (5 by P/D and 1 by EPP), 2 had a partial P/D for intraoperative findings of mediastinal invasion (n=1) or an isolated area of chest wall invasion precluding feasible resection (n=1), and 1 had ET for diffuse chest wall invasion.

Reorganization of the tumor-immune contexture

Evaluable matched tumor and blood, before and after ICB, were available for 15 of the 17 patients receiving ICB and thoracotomy, each of whom had a resection. The single patient undergoing ET in combination group did not have sufficient tumor collected, and the single patient in the monotherapy group undergoing ET had tumor obtained but its quality was later found to be insufficient. Thus, multiplexed imaging mass cytometry (IMC) was performed on pre- and post-ICB tumor samples in an evaluable cohort of 15 patients and demonstrated that a single cycle of monotherapy or combination therapy substantively reorganized the cellular immune contexture of MPM (Figure 1C, Supplementary Figure 2, Supplementary Figure 3).

The frequency of intratumoral CD8 T cells increased following both ICB regimens, the frequency of regulatory T cells (Treg) increased after monotherapy, and there were no statistically significant changes of CD8/Treg ratios following either ICB regimen (Figure 1D). The proportion of memory CD8 T cells ($CD3^+CD8^+CD45RO^+$) increased in MPM tumors only after combination ICB, as did B cells ($CD20^+$) and M1-like tumor-associated macrophages (TAMs) ($CD68^+CD163^-Lysozyme^+$) (Figure 1E). No changes were observed after either ICB regimen in the frequencies of CD4 T cells, $ICOS^+$ CD4 T cells, NK cells, M2-like TAMs, dendritic cells, cancer-associated fibroblasts, stromal cells, or endothelial cells (Supplementary Figure 4). PD-L1 expression on cancer cells did not change following ICB in either group but increased on endothelial cells after monotherapy and combination therapy, and on M1-like TAMs following combination therapy (Figure 1F).

Survival

OS and DFS were evaluated primarily on an intent-to-treat basis in all randomized patients (n=24) and were evaluated at a median of 34.1 months following randomization. Compared with monotherapy, patients treated with combination ICB had longer OS and DFS (P=0.040 and P=0.009, respectively, Figure 2A). Median OS and DFS were 14.0 and 8.4 months in the monotherapy group, respectively, and not reached in the combination group. In the subgroup of patients undergoing thoracotomy (n=21), those treated with combination ICB had longer OS and DFS than those treated with monotherapy (P=0.041 and P=0.014, respectively, Figure 2B). Median OS and DFS were also 14.0 and 8.4 months, respectively, in the monotherapy group and not reached in the combination therapy group. OS of the

monotherapy group was similar to that of the no ICB group and also similar to that of a historical group of MPM patients treated surgically (n=500) (Supplementary Figure 5A). Although limited by sample size, OS was not different between epithelioid and non-epithelioid MPM patients following either ICB regimen (Supplementary Figure 5B).

Adverse Events

AEs were separated into preoperative and postoperative periods. Preoperative AEs were defined as AEs that occurred after ICB and before surgery, and were observed in 14 of 20 patients (70%). In the monotherapy group, 1 patient developed several grade 3 preoperative AEs (12.5%) including dyspnea, edema, fatigue, and nausea. In the combination therapy group, 3 patients developed grade 3 preoperative AEs (27.3%) and these included non-ST-elevation myocardial infarction, acneiform rash, hyperglycemia, and drug-induced hepatitis (Figure 2C, Supplementary Table 2). No grade 4 or 5 AEs were observed in the preoperative period.

In the 30-day postoperative period, AEs ≥grade 3 occurred in 4 patients; 1 of which occurred in the monotherapy group and 3 of which occurred in the no ICB group (Figure 2D, Supplementary Table 3) and all of which were determined to be related to surgery. There was one in-hospital postoperative mortality in this study. This occurred as right heart failure after right EPP in a patient that received monotherapy, in a patient with pre-existing cardiac disease, and was determined to be related to surgery.

Pathologic response

Formal consensus for quantifying pathologic response (PR) to neoadjuvant therapy of any kind has not been established for MPM.[22, 23] We defined PR as >20% tumor regression, and major pathologic response (MPR) was defined as ≤10% residual viable tumor in the resected tissues, similar to approaches used in lung cancer.[24] The percent of residual viable tumor cells after ICB was scored on hematoxylin and eosin-stained clinical specimens by a board-certified thoracic pathologist (M.R.) blinded to clinical outcomes, using multiple slides from at 2–3 regions of tumor resection specimens. Among the 17 patients that underwent surgical resection after neoadjuvant ICB, any PR was observed in 6 patients (35.3%), 3 receiving monotherapy and 3 receiving combination therapy, and was more frequent in MPM tumors that displayed ≥5% tumor cell expression of PD-L1 (P=0.035, Figure 2E, Supplementary Table 4). Major PR occurred in 2 patients (11.8%), 1 receiving monotherapy and 1 receiving combination therapy, and was characterized by histologic features that included tumor cell necrosis, lymphocyte infiltration, and fibrosis (Figure 2F).

Formation of tertiary lymphoid structures

Tertiary lymphoid structures (TLSs) are aggregates of lymphocytes and antigen-presenting cells within tumor tissues that serve as educational hubs for the development of anti-tumor immune responses. Our IMC analyses demonstrated the presence of intratumoral TLSs in MPM tumors (Figure 3A, Supplementary Table 5) and we observed a significant increase in TLS density following ICB which increased with greater magnitude after combination therapy (Figure 3B). We additionally observed a greater increase in TLS formation in tumors that had PR, and that higher pre-treatment TLS density was associated with PR (Figure

3C, Supplementary Table 4). Characterization of post-treatment TLSs demonstrated that they were comprised of a germinal center of proliferative Ki-67$^+$ B cells surrounded by a CD45RA$^+$ B cell zone and follicular dendritic cells meshwork (Supplementary Figure 6), and contained interspersed T cell zones enriched for CD45RO$^+$ CD4 and CD8 T cells as well as CD45RA$^+$ CD4 and CD8 T cells (Figure 3D–E).

Systemic immune responses

Peripheral immune reactivity to ICB was assessed by time-of-flight mass cytometry (CyTOF) of peripheral blood mononuclear cells (PBMCs) obtained before and after ICB in the evaluable cohort of 15 patients (Supplementary Table 6). CD8 and CD4 T cells highly expressing CD57 (Figure 4A), a carbohydrate epitope associated with cytotoxic activation of CD8[25–27] and CD4 T cells,[28] increased in circulation after combination therapy. These CD57$^+$ T cells were enriched for CD8 and CD4 effector memory T cells (Tem; CD45$^+$CD3$^+$CD45RO$^+$CD45RA$^-$CCR7$^-$) and CD8 and CD4 effector memory T cells that re-express CD45RA (Temra; CD45$^+$CD3$^+$CD45RA$^+$CD45RO$^-$CCR7$^-$CD27$^-$CD28$^-$) which are considered to be a terminally differentiated subset of memory T cells that exhibit high expression of perforin and granzyme B (Figure 4B, Supplementary Figure 7). Deeper phenotyping revealed that CD57$^+$ CD8 Temra was a unique Temra population that overexpressed the immunoregulatory marker TIM-3, and that CD57$^+$ CD4 Temra uniquely overexpressed CD161, PD-1, and CTLA-4 (Supplementary Figure 8).

Systemic immune reactivity to ICB was further investigated by CyTOF in post-treatment bone marrow mononuclear cells (BMMCs) isolated from patients who had routine resection of the 6th rib during thoracotomy (Supplementary Table 7). Striking differences in bone marrow composition were observed in patients who received combination therapy (n=5) compared with those that received monotherapy (n=5), most notably including decreased proportions of hematopoietic stem and progenitor cells (HSPCs; CD34$^+$CD117$^+$Lin$^-$) and decreased proportions of CD57$^+$ T cells that had CD8$^+$ and CD4$^+$ Temra phenotypes (Figure 4C–D, Supplementary Figure 9).

Interface of systemic and local anti-tumor immunity

Given the mobilization of circulating CD57$^+$ memory T cells in response to ICB, we investigated whether CD57$^+$ T cells infiltrate post-ICB MPM tumors. We observed abundant CD57$^+$ T cells within MPM TLSs, in both germinal center and T cell zones. CD57$^+$ T cells in germinal centers were predominantly CD45RO$^+$ CD4 T cells (Figure 5A, Supplementary Table 8), which phenotypes partly overlapped with CXCR5(+)PD-1(+) follicular helper T cells (Supplementary Figure 10, Supplementary Table 9).[28,29] CD57$^+$ T cells within TLS T cell zones were predominantly CD45RO$^+$ and CD45RA$^+$ CD8 T cells (Figure 5A), phenotypes consistent CD8 Tem and CD8 Temra, respectively. We next used CD31 expression to identify high endothelial venules (HEVs) in MPM tumors. HEVs are specialized blood vessels in lymph nodes and other lymphoid organs that recruit lymphocytes and that have recently been shown to be responsible for lymphocyte entry into tumors.[30] We observed that TLSs in MPM tumors were rich in HEVs (Figure 5B) and that these HEVs frequently contained CD57$^+$ memory CD8 T cells (Figure 5B). These data are

highly suggestive that ICB mobilizes specialized subsets of circulating CD57-expressing memory CD8 and CD4 T cells from the bone marrow for their recruitment into tumor TLSs.

Lastly, we performed cluster analyses to explore the relationships of nine major immune cell types within bone marrow, blood, and tumor after ICB, in the subset of patients in whom CyTOF could be performed in matched BMMCs, PBMCs, and tumor single cells (n=5), two of whom had PR and TLS formation (responders) and three of whom had neither (non-responders) (Figure 5C). Uniform manifold approximation and projection (UMAP) was used for dimensionality reduction and for visualizing similarities among the differentiation states of immune cells populations within the 3 compartments. In responders, we observed a dynamic immune circuit in which post-ICB BMMC contained heterogenous lymphocyte populations with protein expression profiles more similar to post-ICB PBMC than pre-ICB PBMC; and where CD8 and CD4 T cells with Tem and Temra phenotypes were present in bone marrow, blood, and tumors after ICB. Additionally, in responders, BMMCs shared a large complement of lineage markers with Temra, Tem, B cells, and NK cells, suggesting higher rates of HSPC differentiation into mature multi-lineage lymphocytes. In contrast, a stagnant immune circuit was observed in non-responders, characterized by a myeloid cell-rich bone marrow compartment with minimal variability in HSPC and immune cell differentiation in bone marrow, blood, and tumor; and the absence of mobilization of Tem and Temra from blood to tumor. Taken together, our data support a paradigm in which effective ICB generates *de novo* systemic immune responses that originate in the bone marrow and extend to the tumor microenvironment (Supplementary Figure 11).

DISCUSSION

Preclinical studies have demonstrated that tumor-specific T cell immunity is enhanced when ICB is administered in the neoadjuvant rather than adjuvant setting and substantiate the clinical effectiveness of neoadjuvant ICB in recent trials.[31–33] MPM is a unique tumor that grows along pleural surfaces and that cannot be controlled surgically to a microscopically negative margin. Consequently, residual microscopic disease results in local relapse in more than 75% of cases within just over a year following resection.[34] We reasoned that a neoadjuvant ICB strategy for patients with MPM could leverage the greater burden of tumor antigens that is present before resection to augment systemic immune responses against residual microscopic disease, while avoiding delivery of immunotherapy in the immunosuppressed postoperative state.

In patients with resectable MPM, we show that a single cycle of durvalumab and tremelimumab delivered in the neoadjuvant setting profoundly reorganizes the immune contexture of MPM tumors, and generates memory T cell responses systemically in peripheral immune compartments and locally within MPM tumors. Studies designed with primary clinical endpoints will be needed to confirm the survival impact of neoadjuvant ICB in MPM, however our data showing lower rates of recurrence and longer survival in patients treated with dual agent ICB are provocative and supported by the favorable impact that this regimen had on systemic immunity.

Immune checkpoint inhibitors have traditionally been thought to act, at least in part, by reinvigorating exhausted or dysfunctional tumor-reactive CD8 T cells,[35, 36] however emerging evidence has demonstrated that effective immunotherapy drives new immune responses, rather than reinvigorates pre-existing responses.[37] This concept is supported by data indicating that most tumor-infiltrating T cells subsist in a late dysfunctional state that is resistant to immunotherapeutic reprogramming, and recent studies showing that the fraction of tumor-infiltrating T cells that can be rescued by ICB are those that have recently entered the tumor from the circulation.[38, 39] Further, several reports have demonstrated that blockade of PD-1 or PD-L1 drives novel T cell clones into tumors that were not present prior to ICB.[38, 39] Whereas it is currently poorly understood how local and systemic T-cell immunity collaborate in anti-tumor immunity, clinically effective responses to ICB likely require coordinated activation of both local and systemic T cell reactions against tumor cells in order to result in tumor elimination and prevent recurrence and/or metastases. Our results provide novel insight into the generation of *de novo* systemic immune responses by ICB and suggest that they may begin in the bone marrow and extend to the local tumor microenvironment.

In patients with MPM, we found that combining anti-PD-L1 and anti-CTLA-4 therapy mobilized populations of CD57-expressing CD8 and CD4 effector memory T cells from the bone marrow to the circulation. We identified CD57-expressing CD8 and CD4 T cells in MPM tumors and found $CD57^+$ CD8 memory T cells within HEVs of MPM TLSs, supporting their migration from the peripheral blood. CD57 expression on T cells has been associated with repetitive antigen stimulation in viral infections where $CD57^+$ CD8 T cells highly express interferon-gamma, granzyme B, and perforin,[40] however the role of CD57 on T cells in cancer is less clear. In patients with oral squamous cell carcinoma, $CD57^+$ CD8 T cells possessed potent anti-tumor function and were associated with improved clinical outcomes[41]; and in patients with non-small cell lung cancer, circulating $CD57^+$ CD8 T cells had enhanced cytotoxicity but displayed a terminally differentiated phenotype and impaired proliferative capability.[26] Our data show that the circulating $CD57^+$ T cells that increased after dual agent ICB were largely comprised of CD8 and CD4 Temra. Importantly, in a recent report of patients with unresectable MPM that were treated with nivolumab and ipilimumab, pre-treatment CD8 Temra blood counts were higher in responders than non-responders and were speculated to be effector T cells that were activated by ICB.[42] Taken together, sufficient rationale is provided for further investigation of CD57 as a peripheral biomarker of local and systemic responses to ICB in prospective trials.

The bone marrow is an important and understated contributor to the maintenance of lymphocyte memory and has been proposed as an organ that supports antigen-independent proliferation of recirculating memory T cells. “Recirculating” memory T cells are a loosely defined population of patrolling T cells that circulate through the lymphatic system and blood; migrate in and out of lymph nodes, bone marrow, and non-lymphoid tissues; and orchestrate widespread systemic memory responses.[43, 44] In support of this concept, antigen-specific T cells have been identified in the bone marrow of patients with solid tumors, and in some cases with higher frequency than matched peripheral blood.[45, 46] Based upon our findings, it is reasonable to submit that CD57 could be a marker for recirculating tumor-associated antigen- or neoantigen-specific memory T cells and that the bone marrow could

serve as a reservoir for these $CD57^+$ cells, sheltering them from the harsh environmental conditions of MPM tumors until they are called upon by ICB therapy. More provocative, our single-cell data in matched tumor, blood, and bone marrow suggest that effective ICB responses potentially originate from a dynamic lymphoid reorganization of the bone marrow and that culminates in tactical systemic and local memory T cell responses.

We have previously reported that the cellular immune composition of MPM tumors associated with sensitivity to PD-1 inhibition[47] and our current study shows that the spatial immunologic architecture of MPM is a determinant of tumor pathologic response to PD-L1 plus CTLA-4 inhibition. Pathologic response is a useful surrogate for the efficacy of neoadjuvant ICB in early phase trials[48] and is used clinically in many human cancers to estimate long-term prognosis. Not yet reported for MPM, we show that a single cycle of ICB results in a pathologic response in 35% of MPM tumors and has a major pathologic response rate of 12%. Consistent with recent reports correlating tumor TLS density and clinical response to ICB in other human malignancies,[49–50] MPM tumors that had pathologic responses were rich in TLSs, suggesting that these tumors may already be generating an anti-tumor immune response that is potentially enhanced by ICB. Whereas the importance of TLS-associated B cells in the clinical effectiveness of ICB has been revealed recently in melanoma, sarcoma, and urothelial cancers,[49–52] our understanding of the role of TLS-associated T cells in anti-tumor immunity is relatively limited. Our data indicate that TLSs in MPM are comprised of a distinct T cell zone of CD8 and CD4 tissue-resident memory T cells and form in response to effective ICB, supporting a novel mechanism for the generation of local anti-tumor immunity during effective immunotherapy.

The sample size of our trial limits interpretation of its secondary endpoint clinical outcomes and our results are limited to patients with resectable disease, which tends to favor earlier clinical stage. The no ICB group was used as a benchmark for secondary endpoints of survival was bolstered by historical data from a large cohort of similarly-treated surgical patients, however determining the impact of neoadjuvant ICB will require trials designed with primary survival endpoints. Although this study randomized patients to receipt of prior chemotherapy and MPM subtype histology, both of these variables are potential confounding variables that should be addressed in future studies. For example, 3 patients on study received chemotherapy before enrollment (2 in the no ICB group and 1 in the combination group) and it is possible that receiving chemotherapy before ICB could influence the immunologic and biologic behavior of MPM tumors. Our trial also included patients that were somewhat enriched for non-epithelial tumors, which both demonstrate different clinical behavior than epithelial tumors, and that can overexpress PD-L1. Additionally, although not significantly different between our treatment groups, metabolic activity on PET-CT could be of interest to study as a predictor of response to neoadjuvant ICB. Despite these limitations, to our knowledge, this is the first prospective randomized study of neoadjuvant ICB in MPM. Important for considering future adoption of neoadjuvant ICB for patients with MPM is the safety and feasibility data from this trial: the rate of preoperative adverse events, albeit to only 1 cycle of ICB, was not limiting, and 85% of patients receiving ICB underwent planned thoracotomy without delay.

In conclusion, neoadjuvant anti-PD-L1 and anti-CTLA-4 therapy is biologically active in patients with MPM and stimulates concerted local and systemic effector memory T lymphocyte responses. Neoadjuvant ICB appears safe and feasible in patients with MPM, results in pathologic tumor responses, and has a potentially favorable impact on survival.

Supplementary Material

Refer to Web version on PubMed Central for supplementary material.

ACKNOWLEDGEMENTS

This work was supported by AstraZeneca (Burt), an NIH R37 MERIT Award (Burt: R37CA248478), a Cancer Prevention and Research Institute of Texas grant (Lee: CPRIT RP200443), Michael E. DeBakey Department of Surgery seed grant (Lee), and the Gutenstein Family Foundation (Burt). This project was also supported by the Cytometry and Cell Sorting Core at Baylor College of Medicine with funding from the NIH (NCI P30CA125123 and NCRR S10RR024574) and CPRIT (RP180672) and the assistance of Joel M. Sederstrom. This research was performed in the Flow Cytometry & Cellular Imaging Facility, which is supported in part by the National Institutes of Health through M.D. Anderson's Cancer Center Support Grant CA016672, the NCI's Research Specialist 1 R50 CA243707-01A1, and a Shared Instrumentation Award from the CPRIT RP121010. Dr. Amos is a CPRIT Research Scholar, supported by RR170048. A part of contents was presented at the 101st Annual Meeting of the American Association of Thoracic Surgery in 2021.

Abbreviations

AEs	adverse events
BMMCs	bone marrow mononuclear cells
CTLA-4	cytotoxic T-lymphocyte–associated antigen-4
CyTOF	time-of-flight mass cytometry
EPP	extrapleural pneumonectomy
ET	exploratory thoracotomy
FDA	Food and Drug Administration
HEVs	high endothelial venules
HIOC	heated intraoperative chemotherapy
HSPCs	hematopoietic stem and progenitor cells
ICB	immune checkpoint blockade
IMC	imaging mass cytometry
MCR	macroscopic complete resection
MPM	malignant pleural mesothelioma
NK	Natural killer
OS	overall survival

P/D	pleurectomy/decortication
PBMCs	peripheral blood mononuclear cells
PD-1	programmed cell death-1
PD-L1	programmed cell death-ligand 1
PFS	progression-free survival
PR	pathologic response
TAMs	tumor-associated macrophages
Temra	effector memory T cells re-expressing CD45RA
TLSs	tertiary lymphoid structures
Treg	regulatory T cells
UMAP	uniform manifold approximation and projection

REFERENCES

1. Nelson DB, Rice DC, Niu J, et al. Long-Term Survival Outcomes of Cancer-Directed Surgery for Malignant Pleural Mesothelioma: Propensity Score Matching Analysis. J Clin Oncol 2017:JCO2017738401.
2. Musk AW, Olsen N, Alfonso H, et al. Predicting survival in malignant mesothelioma. Eur Respir J 2011;38:1420–1424. [PubMed: 21737558]
3. Taioli E, Wolf AS, Camacho-Rivera M, et al. Determinants of Survival in Malignant Pleural Mesothelioma: A Surveillance, Epidemiology, and End Results (SEER) Study of 14,228 Patients. PLoS One 2015;10:e0145039. [PubMed: 26660351]
4. Merritt N, Blewett CJ, Miller JD, et al. Survival after conservative (palliative) management of pleural malignant mesothelioma. J Surg Oncol 2001;78:171–174. [PubMed: 11745800]
5. Vogelzang NJ, Rusthoven JJ, Symanowski J, et al. Phase III study of pemetrexed in combination with cisplatin versus cisplatin alone in patients with malignant pleural mesothelioma. J Clin Oncol 2003;21:2636–2644. [PubMed: 12860938]
6. Zalcman G, Mazieres J, Margery J, et al. Bevacizumab for newly diagnosed pleural mesothelioma in the Mesothelioma Avastin Cisplatin Pemetrexed Study (MAPS): a randomised, controlled, open-label, phase 3 trial. Lancet 2016;387:1405–1414. [PubMed: 26719230]
7. Rusch VW, Rosenzweig K, Venkatraman E, et al. A phase II trial of surgical resection and adjuvant high-dose hemithoracic radiation for malignant pleural mesothelioma. J Thorac Cardiovasc Surg 2001;122:788–795. [PubMed: 11581615]
8. Gomez DR, Hong DS, Allen PK, et al. Patterns of failure, toxicity, and survival after extrapleural pneumonectomy and hemithoracic intensity-modulated radiation therapy for malignant pleural mesothelioma. J Thorac Oncol 2013;8:238–245. [PubMed: 23247629]
9. Sugarbaker DJ, Richards WG, Bueno R. Extrapleural pneumonectomy in the treatment of epithelioid malignant pleural mesothelioma: novel prognostic implications of combined N1 and N2 nodal involvement based on experience in 529 patients. Ann Surg 2014;260:577–580; discussion 580–572. [PubMed: 25203873]
10. Rusch VW, Giroux D, Kennedy C, et al. Initial analysis of the international association for the study of lung cancer mesothelioma database. J Thorac Oncol 2012;7:1631–1639. [PubMed: 23070243]

11. Scherpereel A, Mazieres J, Greillier L, et al. Nivolumab or nivolumab plus ipilimumab in patients with relapsed malignant pleural mesothelioma (IFCT-1501 MAPS2): a multicentre, open-label, randomised, non-comparative, phase 2 trial. Lancet Oncol 2019;20:239–253. [PubMed: 30660609]
12. Quispel-Janssen J, van der Noort V, de Vries JF, et al. Programmed Death 1 Blockade With Nivolumab in Patients With Recurrent Malignant Pleural Mesothelioma. J Thorac Oncol 2018;13:1569–1576. [PubMed: 29908324]
13. Okada M, Kijima T, Aoe K, et al. Clinical Efficacy and Safety of Nivolumab: Results of a Multicenter, Open-label, Single-arm, Japanese Phase II study in Malignant Pleural Mesothelioma (MERIT). Clin Cancer Res 2019;25:5485–5492. [PubMed: 31164373]
14. Calabrò L, Rossi G, Morra A, et al. Tremelimumab plus durvalumab retreatment and 4-year outcomes in patients with mesothelioma: a follow-up of the open label, non-randomised, phase 2 NIBIT-MESO-1 study. Lancet Respir Med 2019;7:969–976.
15. Disselhorst MJ, Quispel-Janssen J, Lalezari F, et al. Ipilimumab and nivolumab in the treatment of recurrent malignant pleural mesothelioma (INITIATE): results of a prospective, single-arm, phase 2 trial. Lancet Respir Med 2019;7:260–270. [PubMed: 30660511]
16. Hassan R, Thomas A, Nemunaitis JJ, et al. Efficacy and Safety of Avelumab Treatment in Patients With Advanced Unresectable Mesothelioma: Phase 1b Results From the JAVELIN Solid Tumor Trial. JAMA Oncol 2019;5:351–357. [PubMed: 30605211]
17. Fennell DA, Ewings S, Ottensmeier C, et al. Nivolumab versus placebo in patients with relapsed malignant mesothelioma (CONFIRM): a multicentre, double-blind, randomised, phase 3 trial. Lancet Oncol 2021;22:1530–1540. [PubMed: 34656227]
18. Baas P, Scherpereel A, Nowak AK, et al. First-line nivolumab plus ipilimumab in unresectable malignant pleural mesothelioma (CheckMate 743): a multicentre, randomised, open-label, phase 3 trial. Lancet 2021;397:375–386. [PubMed: 33485464]
19. Peters S, Scherpereel A, Cornelissen R, et al. First-line nivolumab plus ipilimumab versus chemotherapy in patients with unresectable malignant pleural mesothelioma: 3-year outcomes from CheckMate 743. Ann Oncol 2022;33:488–499. [PubMed: 35124183]
20. Rice D, Rusch V, Pass H, et al. Recommendations for uniform definitions of surgical techniques for malignant pleural mesothelioma: a consensus report of the international association for the study of lung cancer international staging committee and the international mesothelioma interest group. J Thorac Oncol 2011;6:1304–1312. [PubMed: 21847060]
21. Sugarbaker DJ, Gill RR, Yeap BY, et al. Hyperthermic intraoperative pleural cisplatin chemotherapy extends interval to recurrence and survival among low-risk patients with malignant pleural mesothelioma undergoing surgical macroscopic complete resection. J Thoracic Cardiovasc Surg 2013;145:955–963.
22. Flores RM, Krug LM, Rosenzweig KE, et al. Induction chemotherapy, extrapleural pneumonectomy, and postoperative high-dose radiotherapy for locally advanced malignant pleural mesothelioma: a phase II trial. J Thorac Oncol. 2006 May;1(4):289–95. [PubMed: 17409872]
23. Krug LM, Pass HI, Rusch VW, et al. Multicenter phase II trial of neoadjuvant pemetrexed plus cisplatin followed by extrapleural pneumonectomy and radiation for malignant pleural mesothelioma. J Clin Oncol. 2009 Jun 20;27(18):3007–13. [PubMed: 19364962]
24. Hellmann MD, Chaft JE, William WN Jr, et al. Pathological response after neoadjuvant chemotherapy in resectable non-small-cell lung cancers: proposal for the use of major pathological response as a surrogate endpoint. Lancet Oncol. 2014 Jan;15(1):e42–50. [PubMed: 24384493]
25. Wu RC, Hwu P, Radvanyi LG. New insights on the role of CD8(+)CD57(+) T-cells in cancer. Oncoimmunology 2012;1:954–956. [PubMed: 23162769]
26. Huang B, Liu R, Wang P, et al. CD8(+)CD57(+) T cells exhibit distinct features in human non-small cell lung cancer. J Immunother Cancer 2020;8.
27. Kared H, Martelli S, Ng TP, et al. CD57 in human natural killer cells and T-lymphocytes. Cancer Immunol Immunother 2016;65:441–452. [PubMed: 26850637]
28. Alshekaili J, Chand R, Lee CE, et al. STAT3 regulates cytotoxicity of human CD57+ CD4+ T cells in blood and lymphoid follicles. Sci Rep 2018;8:3529. [PubMed: 29476109]
29. Padhan K, Moysi E, Noto A, et al. Acquisition of optimal TFH cell function is defined by specific molecular, positional, and TCR dynamic signatures. Proc Natl Acad Sci U S A 2021;118.

30. Asrir A, Tardiveau C, Coudert J, et al. Tumor-associated high endothelial venules mediate lymphocyte entry into tumors and predict response to PD-1 plus CTLA-4 combination immunotherapy. Cancer Cell 2022;40:318–334. [PubMed: 35120598]
31. O'Donnell JS, Hoefsmit EP, Smyth MJ, et al. The Promise of Neoadjuvant Immunotherapy and Surgery for Cancer Treatment. Clin Cancer Res 2019;25:5743–5751. [PubMed: 31040150]
32. Topalian SL, Taube JM, Pardoll DM. Neoadjuvant checkpoint blockade for cancer immunotherapy. Science 2020;367.
33. Cascone T, William WN, Weissferdt A, et al. Neoadjuvant nivolumab or nivolumab plus ipilimumab in operable non-small cell lung cancer: the phase 2 randomized NEOSTAR trial. Nat Med 2021;27:504–514. [PubMed: 33603241]
34. Baldini EH, Richards WG, Gill RR, et al. Updated patterns of failure after multimodality therapy for malignant pleural mesothelioma. J Thoracic Cardiovasc Surg 2015;149:1374–1381.
35. Im SJ, Hashimoto M, Gerner MY, et al. Defining CD8+ T cells that provide the proliferative burst after PD-1 therapy. Nature 2016;537:417–421. [PubMed: 27501248]
36. Paley MA, Kroy DC, Odorizzi PM, et al. Progenitor and terminal subsets of CD8+ T cells cooperate to contain chronic viral infection. Science 2012;338:1220–1225. [PubMed: 23197535]
37. Hiam-Galvez KJ, Allen BM, Spitzer MH. Systemic immunity in cancer. Nat Rev Cancer 2021;21:345–359. [PubMed: 33837297]
38. Wu TD, Madireddi S, de Almeida PE, et al. Peripheral T cell expansion predicts tumour infiltration and clinical response. Nature 2020;579:274–278. [PubMed: 32103181]
39. Yost KE, Satpathy AT, Wells DK, et al. Clonal replacement of tumor-specific T cells following PD-1 blockade. Nat Med 2019;25:1251–1259. [PubMed: 31359002]
40. Focosi D, Bestagno M, Burrone O, et al. CD57+ T lymphocytes and functional immune deficiency. J Leukoc Biol 2010;87:107–116. [PubMed: 19880576]
41. Fang J, Li X, Ma D, et al. Prognostic significance of tumor infiltrating immune cells in oral squamous cell carcinoma. BMC Cancer 2017;17:375. [PubMed: 28549420]
42. Mankor JM, Disselhorst MJ, Poncin M, et al. Efficacy of nivolumab and ipilimumab in patients with malignant pleural mesothelioma is related to a subtype of effector memory cytotoxic T cells: Translational evidence from two clinical trials. EBioMedicine 2020;62:103040. [PubMed: 33166791]
43. Gitto S, Natalini A, Antonangeli F, et al. The Emerging Interplay Between Recirculating and Tissue-Resident Memory T Cells in Cancer Immunity: Lessons Learned From PD-1/PD-L1 Blockade Therapy and Remaining Gaps. Frontiers Immunol 2021;12:755304.
44. Di Rosa F, Pabst R. The bone marrow: a nest for migratory memory T cells. Trends Immunol 2005;26:360–366. [PubMed: 15978522]
45. Safi S, Yamauchi Y, Stamova S, et al. Bone marrow expands the repertoire of functional T cells targeting tumor-associated antigens in patients with resectable non-small-cell lung cancer. Oncoimmunology 2019;8:e1671762. [PubMed: 31741774]
46. Schmitz-Winnenthal FH, Volk C, Z'Graggen K, et al. High frequencies of functional tumor-reactive T cells in bone marrow and blood of pancreatic cancer patients. Cancer Res 2005;65:10079–10087. [PubMed: 16267034]
47. Lee HS, Jang HJ, Choi JM, et al. Comprehensive immunoproteogenomic analyses of malignant pleural mesothelioma. JCI insight 2018;3.
48. Forde PM, Chaft JE, Smith KN, et al. Neoadjuvant PD-1 Blockade in Resectable Lung Cancer. N Engl J Med 2018;378:1976–1986. [PubMed: 29658848]
49. Helmink BA, Reddy SM, Gao J, et al. B cells and tertiary lymphoid structures promote immunotherapy response. Nature 2020;577:549–555. [PubMed: 31942075]
50. Cabrita R, Lauss M, Sanna A, et al. Tertiary lymphoid structures improve immunotherapy and survival in melanoma. Nature 2020;577:561–565. [PubMed: 31942071]
51. van Dijk N, Gil-Jimenez A, Silina K, et al. Preoperative ipilimumab plus nivolumab in locoregionally advanced urothelial cancer: the NABUCCO trial. Nat Med 2020;26:1839–1844. [PubMed: 33046870]

52. Gao J, Navai N, Alhalabi O, et al. Neoadjuvant PD-L1 plus CTLA-4 blockade in patients with cisplatin-ineligible operable high-risk urothelial carcinoma. Nat Med 2020;26:1845–1851. [PubMed: 33046869]

TRANSLATIONAL RELEVANCE STATEMENT

Immune checkpoint blockade (ICB) with nivolumab and ipilimumab has become standard treatment for patients with unresectable malignant pleural mesothelioma (MPM). However, the impact of neoadjuvant ICB in MPM has not yet been evaluated. We report the results of a randomized, phase 2, window-of-opportunity trial of neoadjuvant durvalumab versus durvalumab plus tremelimumab followed by surgery in patients with resectable MPM. A neoadjuvant ICB strategy is feasible and safe for patients with MPM and results in tumor pathologic response in 35% of patients. Patients receiving neoadjuvant dual immunotherapy had statistically longer overall and progression-free survival than those receiving durvalumab alone. Integrated single-cell profiling revealed that combination ICB remodeled the immune contexture of tumors and mobilized effector memory T cells from the bone marrow to the circulation. These data indicate that neoadjuvant durvalumab plus tremelimumab orchestrates *de novo* systemic immune responses that extend to the tumor microenvironment and correlate with favorable outcomes.

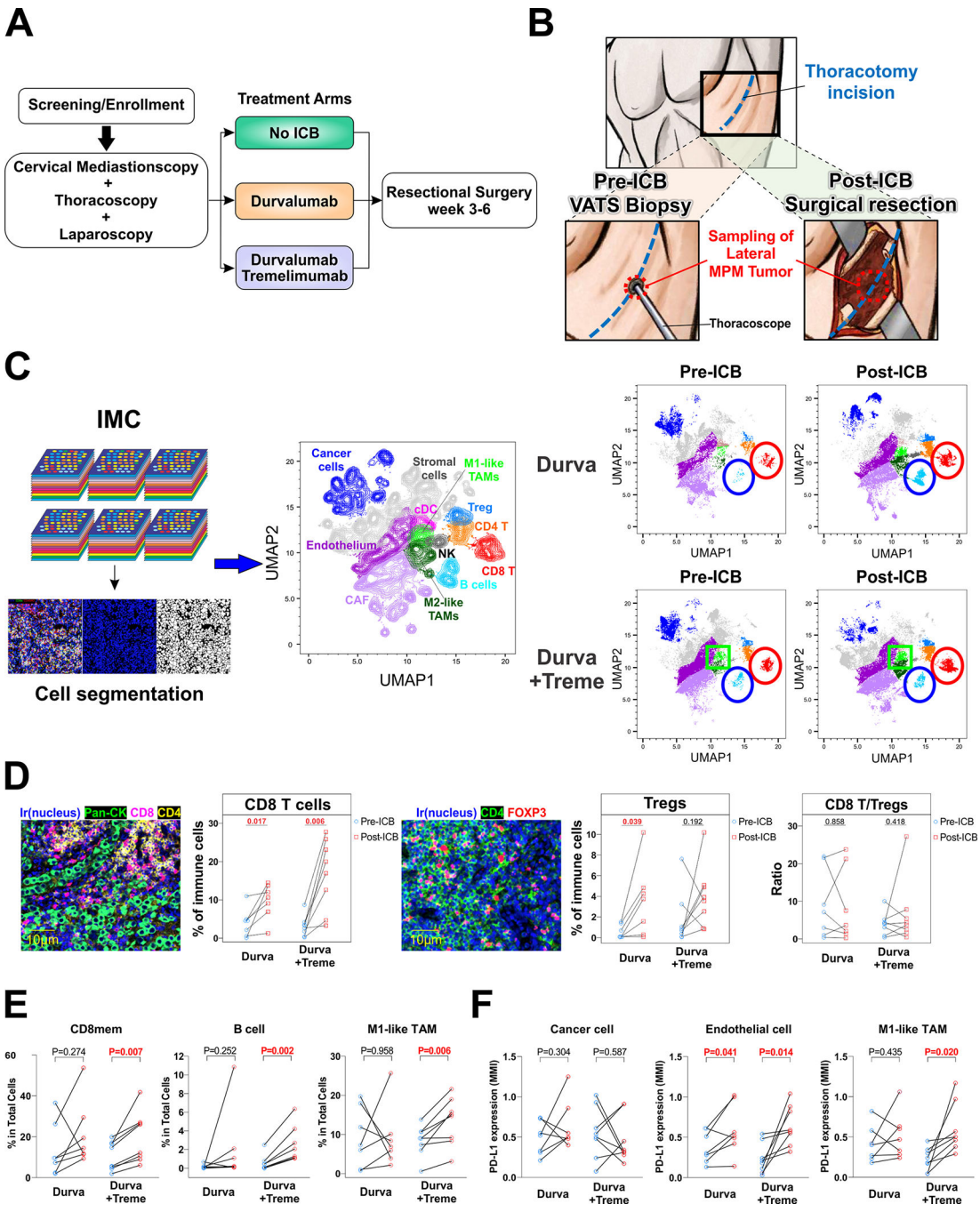

Figure 1. Reorganization of the tumor-immune contexture by neoadjuvant ICB.

A. Trial Schema. **B.** Tissue procurement before and after ICB. **C**. Imaging mass cytometry (IMC) was performed on surgically obtained tumor sections before and after ICB using 35 markers and displayed as uniform manifold approximation and projection (UMAP) plot representations of the tumor-immune microenvironment. The red circle outlines CD8 T cells, the blue circle highlights B cells, and the green square outlines M1-like TAMs. **D**. Primary endpoint of change in CD8/Treg ratio following dual agent neoadjuvant ICB. **E**. Cell populations whose frequencies significantly changed following neoadjuvant ICB are

shown. **F**. PD-L1 alteration on cancer cells, endothelial cells, and M1-like TAM following neoadjuvant ICB.

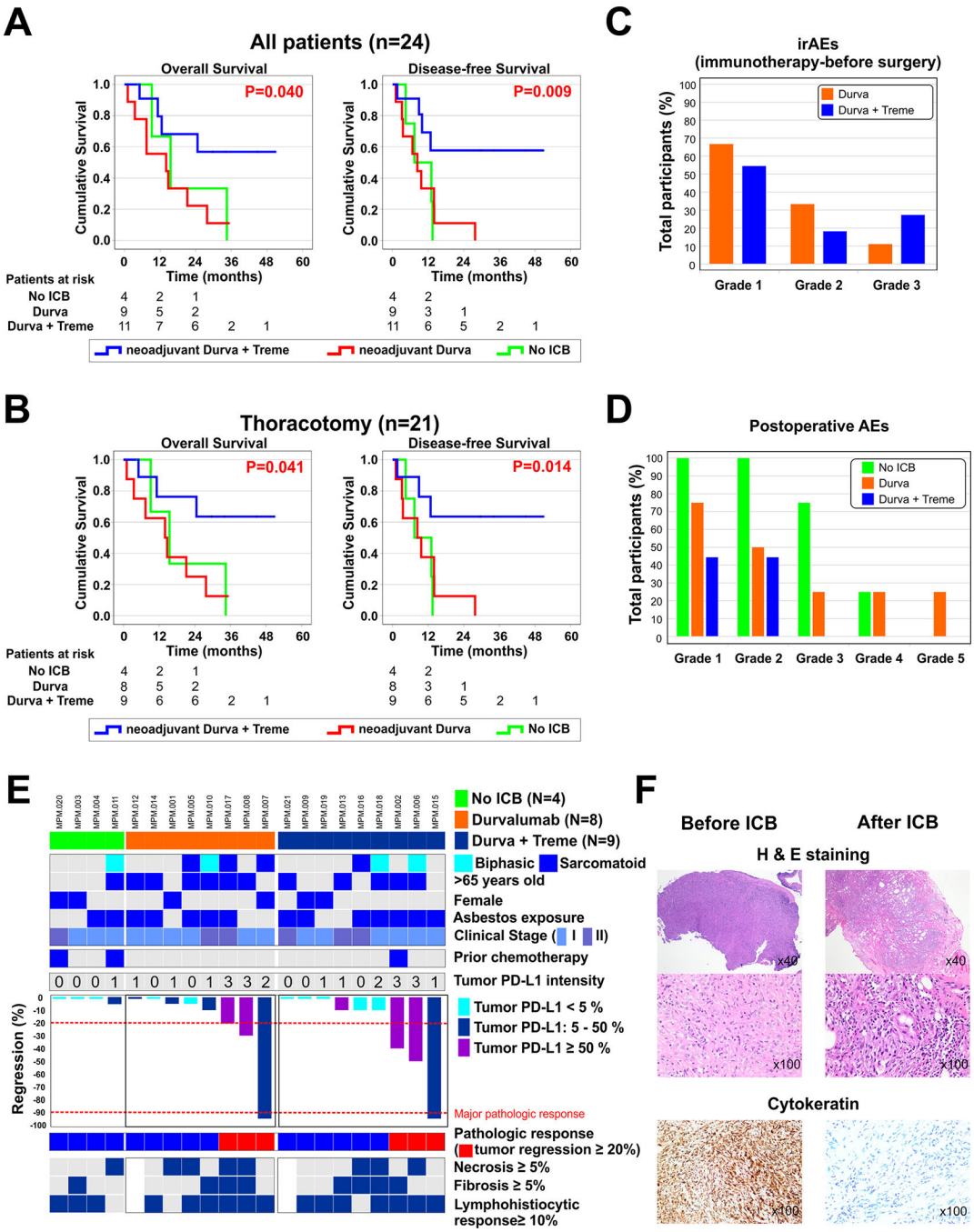

Figure 2. Clinical endpoints of patients receiving neoadjuvant ICB.

A. Overall survival (OS) and disease-free survival (DFS) are shown for all patients receiving ICB (n=24). **B.** OS and DFS for the subgroup of patients receiving ICB and having thoracotomy (n=21). P-values were generated from the comparison of survival between the monotherapy and combination therapy groups using log-rank tests. **C**. Preoperative adverse events (AEs) were defined as AEs before surgery. No grade 4–5 irAEs were observed. **D**. Postoperative AEs within 30 days following surgery are shown. **E**. Patient characteristics and details of pathologic response (PR). We defined PR as >20% tumor regression, and

major pathologic response (MPR) as ≤10% residual viable tumor in the resected tissues. Among the 17 patients that underwent surgical resection after neoadjuvant ICB, PR was observed in 6 patients (35.3%), 3 receiving monotherapy and 3 receiving combination therapy. MPR occurred in 2 patients (11.8%), 1 receiving monotherapy and 1 receiving combination therapy. **F**. H&E and immunohistochemistry findings in a representative tumor with major pathologic response.

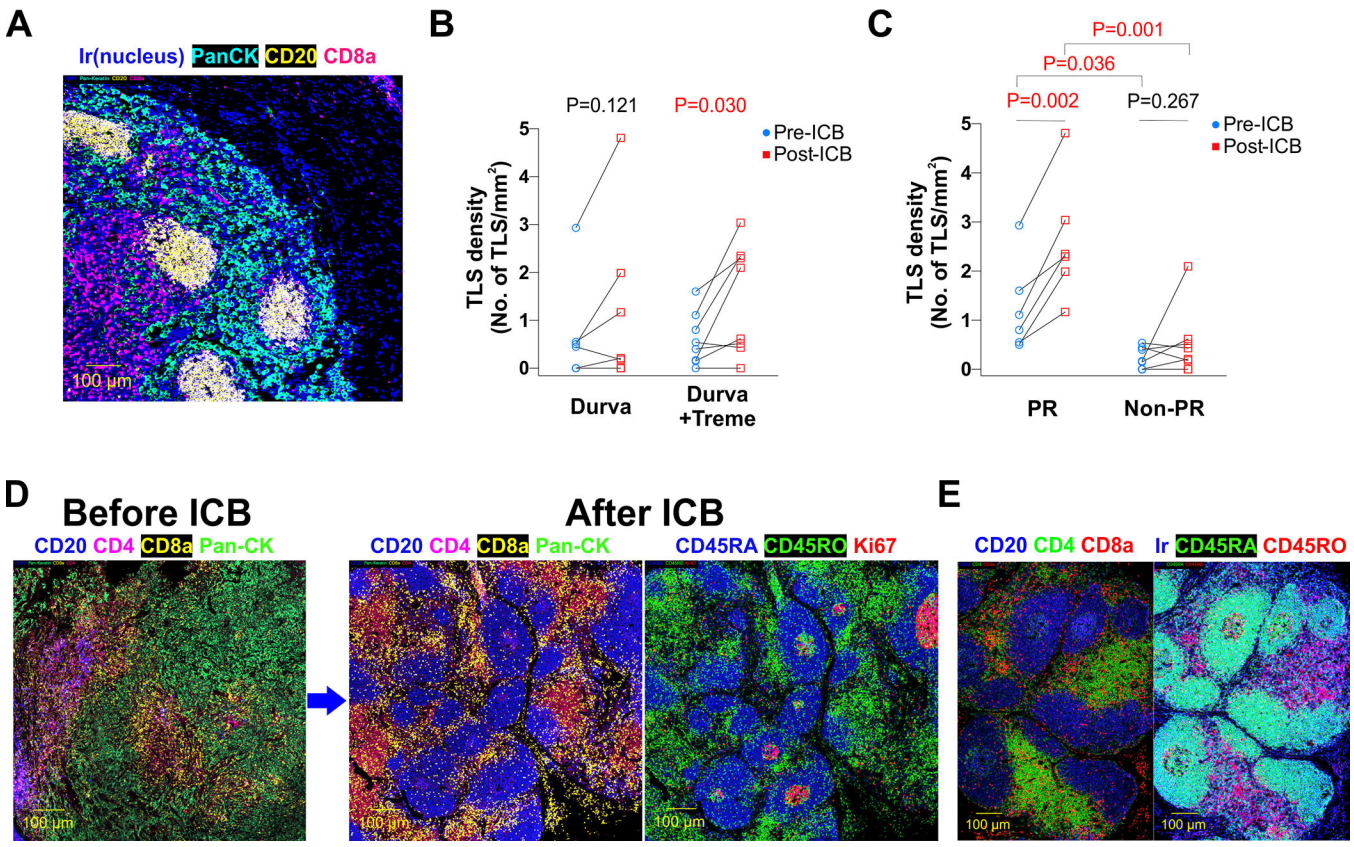

Figure 3. Formation of tertiary lymphoid structures after neoadjuvant ICB.

A. Representative IMC images demonstrating the presence of intratumoral tertiary lymphoid structures (TLSs) in MPM tumors. **B**. TLS density before and after durvalumab and durvalumab plus tremelimumab. **C**. TLS density before and after ICB, stratified by tumors that had pathologic response (PR) or no PR. **D**. IMC images of an MPM tumor from a patient receiving durvalumab and tremelimumab demonstrate induction of TLSs from ICB. **E.** IMC dissection of TLS composition revealed enrichment for $CD45RO^{+}$ and $CD45RA^{+}$ CD4 and CD8 T cells.

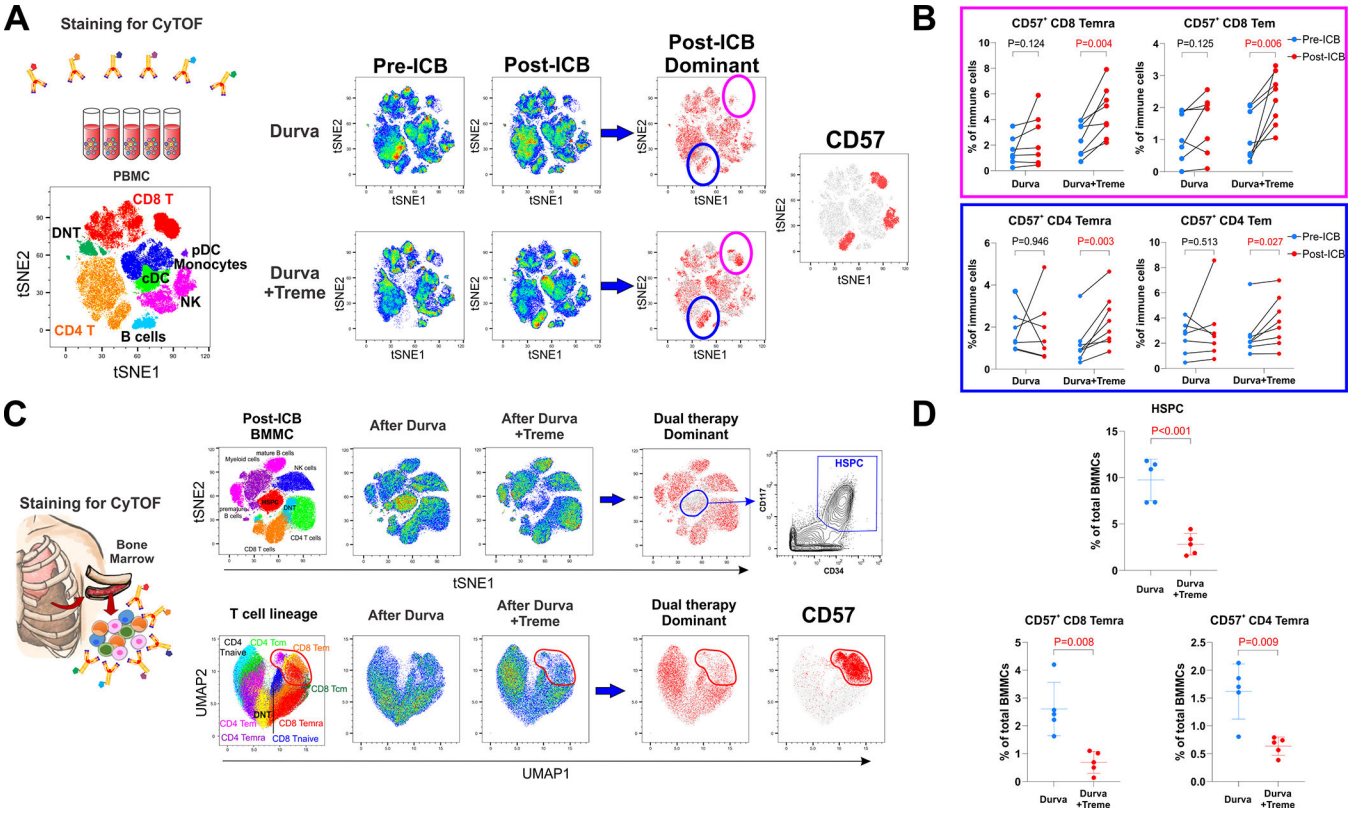

Figure 4. Activation of systemic immunity by neoadjuvant ICB.

A. Dynamic changes in PBMCs after durvalumab monotherapy (n=7) and combination durvalumab plus tremelimumab (n=8). Post-ICB dominant plots compare pre-ICB and post-ICB cell populations to display major changes in cell population frequencies that occur from ICB therapy. A plot of CD57 expression on all cells is provided as a reference for the post-ICB dominant plots and together show that the two dominant cell populations that increased after combination ICB were CD8 and CD4 T cells that express CD57. **B**. Circulating $CD57^+$ CD8 effector memory T cells (Tem), $CD57^+$ CD8 effector memory T cell re-expressing CD45RA (Temra), $CD57^+$ CD4 Tem, and $CD57^+$ CD4 Temra increased after combination ICB. **C**. Bone marrow mononuclear cells (BMMCs) were obtained from ribs resected for surgical exposure following durvalumab (n=5) and durvalumab plus tremelimumab (n=5). Dual therapy dominant plots demonstrate a decrease in hematopoietic stem and progenitor cells (HSPCs) and a decrease in $CD57^+$ T cells following combination ICB. A contour plot of HSPC and a dot plot of $CD57^+$ T cells are provided for reference. **D**. Combination ICB decreased bone marrow populations of cells with $CD57^+$ CD8 Temra and $CD57^+$ CD4 Temra phenotypes.

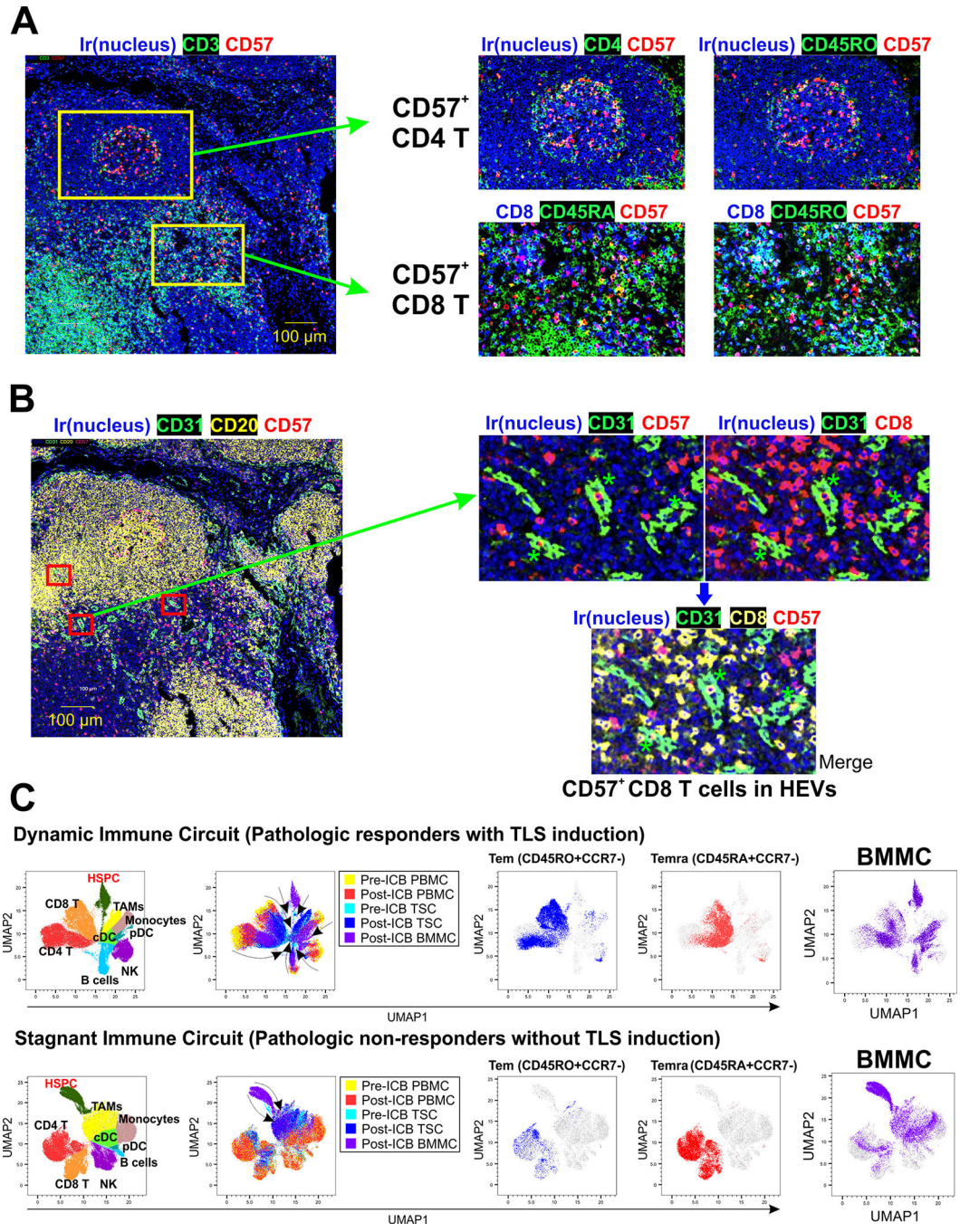

Figure 5. Interface of systemic and local anti-tumor immunity.

A. Identification of CD57$^+$ T cells in the tumor immune environment after ICB. CD57$^+$ T cells were located in germinal center areas and T cell zones of MPM TLSs. CD57$^+$ T cells in germinal centers were CD45RO$^+$ CD4 T cells. CD57$^+$ T cells in T cell zones contained CD45RA$^+$ and CD45RO$^+$ CD8 T cells, consistent with CD8 Temra and CD8 Tem, respectively. **B**. Identification of CD57$^+$ CD8 T cells in high endothelial venules (HEVs) expressing CD31 (marked with red rectangles in the lower magnification figure on the left, and with green asterisks on the higher magnification figure on the right).

Higher magnification views demonstrate $CD57^+$ T cells in HEVs. **C**. Cluster analysis of major cell types within the matched bone marrow, blood, and tumors was performed with CyTOF in 2 responders to ICB (PR and TLS formation) and 3 non-responders (no PR and no TLS formation). We observed a dynamic interaction between systemic and local immunity in responders (dynamic immune circuit), shown as the convergence of immune cell differentiation states from pre-ICB PBMC into post-ICB tumor cells, including CD8 and CD4 Tem and Temra; and HSPC differentiation into mature multilineage cells including Temra and Tem. In contrast, a “stagnant immune circuit” was observed in non-responders, with unchanged differentiation states of circulating and tumor-infiltrating immune cells after ICB, failure of Temra recruitment into the tumor, and abundant HSPC and myeloid cells in the bone marrow.

Table 1.

Patient Characteristics

Variable	No ICB	Durvalumab	Durvalumab + Tremelimumab	Total	P-value
Randomized Patients					
Number of patients	4	9	11	24	
Age, year	58.8 ± 13.4	67.9 ± 6.1	63.4 ± 9.5	64.3 ± 9.3	0.246
Gender					0.440
Male	2 (50 %)	7 (78%)	9 (82%)	18 (75%)	
Female	2 (50 %)	2 (22%)	2 (18%)	6 (25%)	
Asbestos exposure	2 (50%)	5 (62.5%)	6 (75%)	13 (54%)	0.874
PFT					
FVC	2.1 ± 0.2	2.4 ± 0.5	2.6 ± 0.8	2.4 ± 0.6	0.385
%FVC	60 ± 12	59 ± 17	60 ± 21	60 ± 17	0.992
FEV1	1.8 ± 0.2	1.9 ± 0.4	1.9 ± 0.5	1.9 ± 0.4	0.937
%FEV1	69 ± 15	62 ± 15	57 ± 18	61 ± 16	0.496
FEV1/FVC	89 ± 13	82 ± 9	83 ± 15	83 ± 12	0.647
Clinical stage					0.967
I	3 (75%)	7 (78%)	8 (73%)	18 (75%)	
II	1 (25%)	2 (22%)	3 (27%)	6 (25%)	
Histology					0.531
Epithelioid	3 (75%)	5 (56%)	8 (73%)	16 (67%)	
Biphasic	1 (25%)	1 (11%)	2 (18%)	4 (17%)	
Sarcomatoid	0	3 (33%)	1 (9%)	4 (17%)	
PD-L1 (%)					0.313
0–5%	3 (75%)	3 (33%)	7 (64%)	13 (54%)	
5–50%	1 (25%)	4 (44%)	1 (9%)	6 (25%)	
50–100%	0 (0%)	2 (23%)	3 (27%)	5 (21%)	
SUVmax	5.3 ± 2.7	11.0 ± 8.1	5.7 ± 3.1	7.8 ± 6.1	0.123
Prior chemotherapy	2 (50%)	0 (0%)	1 (9.1%)	3 (12.5%)	1.0 *
irAEs (all grades)	-	7 (78%)	7 (64%)	14 (70%)	0.642 *
Interval from ICB to surgery (days)		25 ± 7 (N=8)	28 ± 14 (N=9)	22 ± 14 (N=17)	0.554 *
Patients undergoing Thoracotomy					
Number of patients	4	8	9	21	
Procedure					0.219

Variable	No ICB	Durvalumab	Durvalumab + Tremelimumab	Total	P-value
EPP	3 (75%)	2 (25%)	1 (11%)	6 (29%)	
P/D	1 (25%)	4 (50%)	5 (56%)	10 (48%)	
Partial P/D	0 (0%)	1 (12.5%)	2 (22%)	3 (14%)	
ET		1 (12.5%)	1 (11%)	2 (9%)	
Operation time (minutes)	419± 165	362±153	347±129	367± 141	0.720
Estimate Blood Loss (L)	0.8 ± 0.6	1.6 ± 1.0	1.1 ± 0.8	1.2 ± 0.9	0.399
Intraoperative transfusion	4 (100%)	6 (75%)	4 (44%)	14 (67%)	0.119
HIOC	4 (100%)	4 (50%)	3 (33.3%)	11 (52%)	0.084
Macroscopic complete resection	4 (100%)	6 (75%)	6 (67%)	16 (76%)	0.817
Length of stay (days)	13.3 ± 2.1	11.4 ± 7.5	11.4 ± 6.5	11.8 ± 6.1	0.873
Histology					0.651
Epithelioid	3 (75%)	4 (50%)	6 (67%)	13 (62%)	
Non-epithelioid	1 (25%)	4 (50%)	3 (33%)	8 (38%)	
Pathologic stage	pstage	ypstage	ypstage		0.986
0	0	1 (12.5%)	1 (11.1%)		
I	4 (100%)	4 (50%)	4 (44.5%)		
II	0	0 (0%)	0 (0%)		
III	0	2 (25%)	3 (33.3%)		
IV	0	1 (12.5%)	1 (11.1%)		
Adjuvant chemotherapy	2 (50%)	3 (38%)	5 (56%)	10 (48%)	0.754
Adjuvant radiotherapy	1 (25%)	1 (12.5%)	0	2 (9.5%)	0.343

* P-values are generated from the comparison of durvalumab to durvalumab + tremelimumab.

EPP, extrapleural pneumonectomy; ET, exploratory thoracotomy; HIOC, heated intraoperative chemotherapy; irAE. immunotherapy-related adverse events; P/D, pleurectomy/decortication; PD-L1, programmed cell death 1 ligand 1; SUVmax, maximum standardized uptake value.